JOURNAL OF CATALYSIS **121**, 375–385 (1990)

On the Properties of Silica-Supported Bimetallic Fe–Cu Catalysts

Part II. Reactivity in the Fischer–Tropsch Synthesis

A. F. H. WIELERS,[1] G. W. KOEBRUGGE, AND J. W. GEUS

Department of Inorganic Chemistry, University of Utrecht, Croesestraat 77a,
3522 AD Utrecht, The Netherlands

Received July 8, 1986; revised August 21, 1989

The catalytic performance of bimetallic Fe–Cu catalysts in the Fischer–Tropsch reaction has been investigated. The results show that due to a higher degree of iron reduction the bimetallic copper-rich Fe–Cu catalysts exhibit a higher activity than the monometallic iron catalysts. At high copper levels the activity (as was expected) strongly decreases. It is argued that under Fischer–Tropsch conditions the surfaces of the bimetallic particles consist of iron–iron carbide islets explaining that the effect of copper on the selectivity (increased production of methane, carbon dioxide, and paraffins instead of olefins) becomes apparent only at high copper contents (above 60 at.%). Carburization studies under more severe conditions show that growth of filamentary carbon proceeds not only on the monometallic iron particles but also on the iron–iron carbide islets present in the surface of the bimetallic particles, thus explaining the formation of very thin whiskers. © 1990 Academic Press, Inc.

INTRODUCTION

The conversion of syngas (CO–H_2 mixtures) to hydrocarbons via the Fischer–Tropsch synthesis has been widely studied. The application of iron-based catalysts in this process has been the subject of numerous investigations (*1–5*). The formation of carbides is a prerequisite for the iron catalysts to exhibit the desired activity and selectivity and the presence of surface carbides and (inactive) bulk carbide has been observed by several investigators (*3–5*). However, extensive carbide formation leads to the growth of, e.g., filamentary carbon (*2*, *6–8*). Owing to the mechanical strength of these whiskers the structure of the catalysts completely disintegrates and, when operating in a fixed-bed reactor plugging of the reactor occurs. It has been proposed (*6–8*) that filamentary carbon growth proceeds at the metal–support interface via a decomposing metastable iron carbide phase. As copper does not react to a carbide, it was anticipated that alloying iron with copper may be effective in reducing whisker growth. On the other hand, it has been established with Ni–Cu catalysts that the Fischer–Tropsch activity of the alloys decreases more than proportionally with the copper concentration (*9–11*). Furthermore, with Ni–Cu alloys it has been shown that at low temperatures the selectivity for the formation of higher hydrocarbons decreases compared to that of the pure nickel catalyst, whereas at higher temperatures it increases (*12*). Thus, with Fe–Cu catalysts the effect of copper on the activity and selectivity needs to be investigated. In this work we will report on a systematic study on the activity, selectivity, and stability of bimetallic Fe–Cu catalysts in the Fischer–Tropsch synthesis (FTS).

From a survey of the literature it emerges that with Fe–Cu alloys no consensus exists on the effect of alloying on activity and selectivity. The precipitated iron catalyst developed by Ruhrchemie and used in the

---

[1] Present address: Koninklijke/Shell Laboratorium, Badhuisweg 3, 1031 CM Amsterdam, The Netherlands.

0021-9517/90 $3.00
Copyright © 1990 by Academic Press, Inc.
All rights of reproduction in any form reserved.

fixed-bed reactors at SASOL contains about 5% wt. Cu. Dry (*2*) states that the addition of copper is to enhance the rate of reduction, allowing lower reduction temperatures and yielding catalysts with a higher activity than monometallic iron catalysts. Shah and Perrotta (*13*) have found that Fe–Cu catalysts afford the formation of a higher amount of C_{5+} (hydrocarbons containing more than five carbon atoms) than does a pure iron catalyst. Anderson (*1*) and Wachs *et al.* (*14*) concluded that the presence of copper does not alter the activity and selectivity. On the other hand, a number of patents have been published claiming that copper markedly enhances the selectivity for oxygenated products (*16*).

Anderson (*1*) and others (*15*) have found that the presence of copper lowers the rate of carbon formation on iron. According to Dry (*2*), however, studies at SASOL have not confirmed this conclusion. Wachs *et al.* (*14*) have also found that the rate of carbon formation is not affected by the presence of copper (or another IB metal such as silver). According to these authors this was a result of a poor contact between the respective metals during the Fischer–Tropsch reaction.

In this work we have set out to investigate the catalytic properties of bimetallic Fe–Cu catalysts in more detail. In Part I (*17*) we have reported on a preparation procedure involving the consecutive precipitation of the metal precursors onto the support by means of deposition–precipitation. Extensive characterization studies of the reduced Fe–Cu catalysts have shown that iron is present as Fe^{2+} ions in an iron(II)silicate phase and that the zero-valent iron atoms are present in monometallic α-Fe particles and as small iron clusters in bimetallic Fe–Cu particles. It was shown that with increasing copper concentration the amount of iron present in the bimetallic Fe–Cu particles increases at the expense of the amount of iron in the monometallic α-Fe particles.

EXPERIMENTAL

The preparation procedure and the characterization experiments have been described in detail in Part I (*17*). Prior to reduction the catalyst samples were air-dried at 393 K for 16 h. Activity and selectivity measurements under atmospheric pressure were performed in a differential fixed-bed reactor (i.d. 10 mm). The composition of the gas phase could be analyzed before and after passage through the reactor. Details of the experimental setup and analyzing system have been described elsewhere (*6*). Fresh catalyst samples (100–250 mg, pellet diameter $0.4 < d < 0.5$ mm) were reduced in a 10 vol.% H_2/N_2 stream for 16 h at 773 K. Subsequently, the samples were flushed with pure nitrogen for 1 h at 723 K before cooling to the reaction temperature (553 K). Next H_2/CO was introduced in the reactor ($H_2/CO = 3.0$, $P(CO) = 0.05$ bar, $P(H_2) = 0.15$ bar, and N_2 as a balance). Under these conditions the main products obtained were C_1–C_3 and only traces of higher hydrocarbons. The measurements were performed at a constant space velocity (8000 ± 200 h^{-1}) and the amount of catalyst was adjusted to keep the total CO conversion below 5% ensuring that rate data were measured under differential conditions. The absence of mass and heat transfer effects were verified with the criteria outlined by Smith (*18*).

Carbon deposition was investigated in the same reactor under more severe conditions in order to enhance the rate of carbon formation and to favour the growth of filamentary carbon. The H_2/CO ratio was $1/3[P(CO) = 0.15$ bar and $P(H_2) = 0.05$ bar], the reaction temperature was 673 K, and the space velocity was (8000 ± 200) h^{-1}. With all samples investigated carbon deposition was carried out under these conditions for 16 h. After such a run the samples were subjected to a forced cool-down in N_2 to room temperature, typically within 2 min, and then analyzed with regard to the deposited carbon. Temperature-programmed hydrogenation (TPH) of these carbon deposits was next performed using 10 vol.% H_2/N_2 at a total flow rate of 1 cm^3/s. The only product observed was methane. Its evolution was discontinuously measured as a function of temperature using GC analysis. Due to the time required for one analysis (7 min) linear heating rates were limited to 0.5 K/min.

Schulz–Flory distributions were obtained from the activity measurements performed at elevated pressure (6 bar). These were performed in a fixed-bed bench-scale reactor at 573 K ($H_2/CO = 3.0$; $P(CO) = 0.30$ bar, $P(H_2) = 0.90$ bar, and N_2 as a balance). With each catalyst investigated the space velocity was always 10,000 ± 300 h^{-1}. Details of the equipment have been described by Kuijpers *et al.* (*19*). The CO conversion was kept below 8% and no temperature rise in the catalyst bed was observed. Under these conditions the main products observed were *n*-hydrocarbons (C_1–C_5). All other measurements were performed in the above-mentioned atmospheric fixed-bed microreactor.

The experimental details of the Mössbauer experiments have been described (*17*). The experiments were carried out in a cell permitting the *in situ* measurements of the spectra under the gas atmosphere used during the pretreatment. A reduced (16 h at 773 K) sample (Fe60Cu40) was carbided in a H_2/CO stream ($H_2/CO = 3$) at either 553 or 673 K. After cooling to room temperature Mössbauer spectra were collected.

Electron microscopy was performed with either a Philips EM 420 or a Jeol 200C electron microscope. Carbided samples were statically passivated in air, ultrasonically treated in ethanol, and dispersed over a holey carbon film.

All gases were supplied by Hoekloos. Hydrogen and nitrogen were successively passed through columns containing a copper catalyst (BASF R 3-11) and a molecular sieve (Linde 4A) to remove traces of oxygen and water, respectively. Carbon monoxide was used without further purification.

Definitions of activity and selectivity are listed below.

r_{C_n} = the rate of formation of hydrocarbons with *n* carbon atoms (nmol s^{-1} mg_{cat}^{-1})

$r_{C_n^{2-}}$ = the rate of formation of olefins with *n* carbon atoms (nmol s^{-1} mg_{cat}^{-1})

r_{CO_2} = the rate of conversion of carbon monoxide to carbon dioxide (nmol s^{-1} mg_{cat}^{-1})

r_{HC} = the rate of conversion of carbon monoxide to hydrocarbons from C_1 to C_n,

$$r_{HC} = \sum_{i=1}^{n} i r_{C_i}$$

$$S_{C_2^{2-}} = r_{C_2^{2-}}/r_{C_2}$$
$$S_{CH_4} = r_{C_1}/r_{HC}$$
$$S_{CO_2} = r_{CO_2}(r_{HC} + r_{CO_2})$$

RESULTS

In Fig. 1 the Fischer–Tropsch activity for the series of bimetallic iron–copper catalysts is shown as a function of the copper content. With all catalysts the activity de-

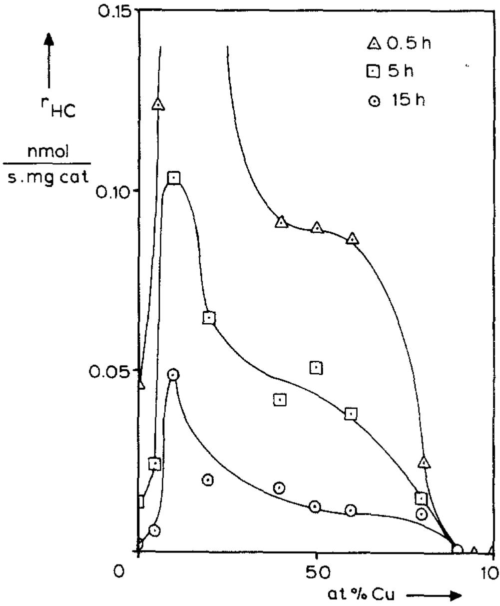

FIG. 1. Rate of hydrocarbon production as a function of the copper content for catalysts which were on stream for 0.5, 5, and 15 h. Not shown in the figure are the initial activities of Fe90Cu10 (0.51 nmol s^{-1} mg_{cat}^{-1}) and Fe80Cu20 (0.32 nmol s^{-1} mg_{cat}^{-1}).

creases with increasing time on stream. It appears that the FT activity passes through a maximum (at 10–20 at.% Cu). The activity of both the iron-rich (<5 at.% Cu) and the copper-rich catalysts (>80 at.% Cu) is very low. The activity of the copper catalyst is nil under these conditions, which is to be anticipated as copper is a poor Fischer–Tropsch catalyst (*20*). Since Fe is a very effective catalyst for this reaction, it is remarkable that the monometallic iron catalyst exhibits a lower activity than the iron-rich bimetallic catalysts. In a previous publication we have shown that the degree of reduction of the reduced Fe/SiO_2 catalyst is rather low (about 20% (*21*)) and furthermore infrared spectra of adsorbed CO on the reduced iron catalyst indicated that the reduced iron particles are (partly) encapsulated by iron(II)silicate, explaining the low Fischer–Tropsch activity of this catalyst (*21*). Infrared spectra of adsorbed CO on reduced bimetallic catalysts showed that iron present in the bimetallic particles is not encapsulated by iron(II)silicate (*17*).

The effect of copper on the chain length distribution (i.e., on the probability of chain growth (α)) can be inferred from the Schulz–Flory plots shown in Fig. 2. Product distributions are calculated for a pure Fe/SiO_2 catalyst which was on stream for 2.5 h and for an Fe–Cu catalyst (overall composition 60 at.% Fe) on stream for 3.5 and 15.75 h, respectively. The activity of the Fe/SiO_2 catalyst was virtually nil after 15 h. It turns out that the probability of chain growth is not markedly affected by (i) the time on stream and (ii) the presence of copper.

In order to evaluate the effect of copper on the selectivities over the entire compositional range, methane, ethene, and carbon dioxide selectivities are given in Figs. 3a–3c. Data are plotted for catalysts that were on stream for 0.5, 5, and 15 h. Only at high copper concentrations do the methane and carbon dioxide selectivities markedly increase, whereas the selectivity for the formation of olefins decreases (data are given for ethene, but the same applies to propene). Thus, the effect of copper on the particular selectivities becomes pronounced only at high copper contents.

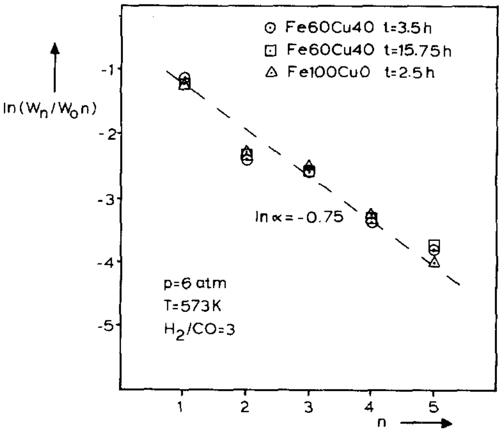

FIG. 2. Schulz–Flory plots for the Fe/SiO_2 and the $Fe60Cu40/SiO_2$ catalysts.

Figure 4 shows room temperature Mössbauer spectra of a bimetallic Fe–Cu catalyst (60 at.% Fe) reduced for 16 h at 773 K and consecutively exposed to syngas at 553 K for 6 h and at 673 K for 6 h. In the spectrum of the reduced catalyst three species are present: (i) iron(II)silicate (doublet), (ii) monometallic α-iron (sextuplet), and (iii) zero-valent iron present as iron clusters in a bimetallic Fe–Cu particle (giving rise to a singlet in the most-negative peak of the above-mentioned doublet). Full details of this particular spectrum are given elsewhere (*17*). Upon exposure of the reduced catalyst to syngas, α-iron is converted to iron carbide (ε'-$Fe_{2.2}C$ and θ-Fe_3C). Furthermore, the peak area of the most-negative peak of the doublet has also decreased (the doublet becomes more symmetric), indicating that part of the iron clusters present in the bimetallic Fe–Cu catalyst also reacts to iron carbide. These features become more pronounced at 673 K. Thus, although iron is present in a bimetallic Fe–Cu particle, copper does not prevent the formation of iron carbide. The parameters and the relative resonant areas

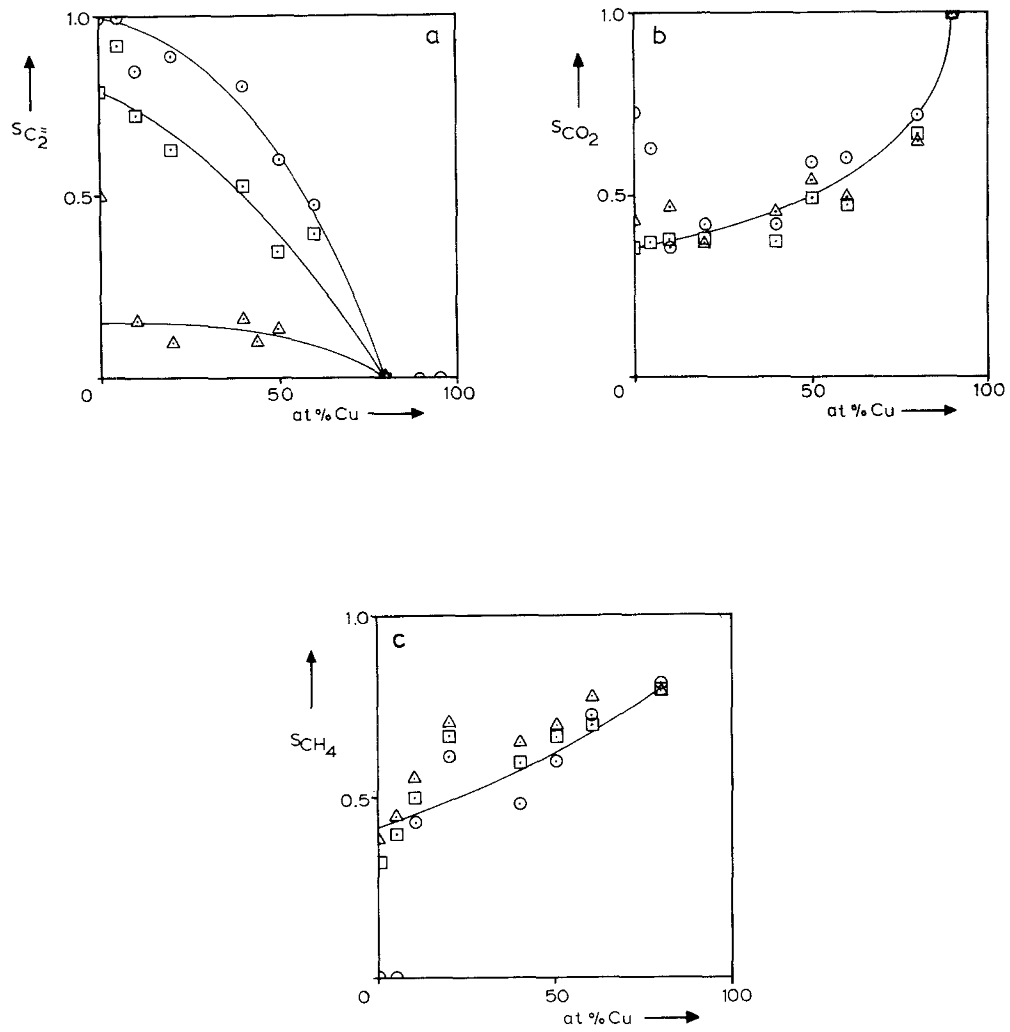

FIG. 3. (a) Ethene, (b) carbon dioxide, and (c) methane selectivities as a function of the copper content for samples on stream for 0.5 (△), 5 (□), and 15 h (○).

that can be deduced from these spectra are given in Table 1. Good fits of the iron carbide contributions could only be obtained by fitting with subspectra of ε'-$Fe_{2.2}C$ and θ-Fe_3C allowing the calculation of the relative contributions of these species in the spectra. The accuracy of these calculations, however, is rather poor and therefore these data should be taken as an indication only. The Mössbauer parameters for the iron carbides involved have been given by Niemantsverdriet *et al.* (*5*).

Finally, we have investigated the tendency of the bimetallic catalysts to grow filamentary carbon. Following the approach by de Bokx *et al.* (*6*) experimental conditions were applied that favour both thermodynamically and kinetically filamentous carbon growth, i.e., a relatively high temperature and a high CO/H_2 ratio (3.0). The space velocity and the time on stream where identical in the carburization experiments carried out with the various catalysts. In Fig. 5 TPH profiles of catalysts

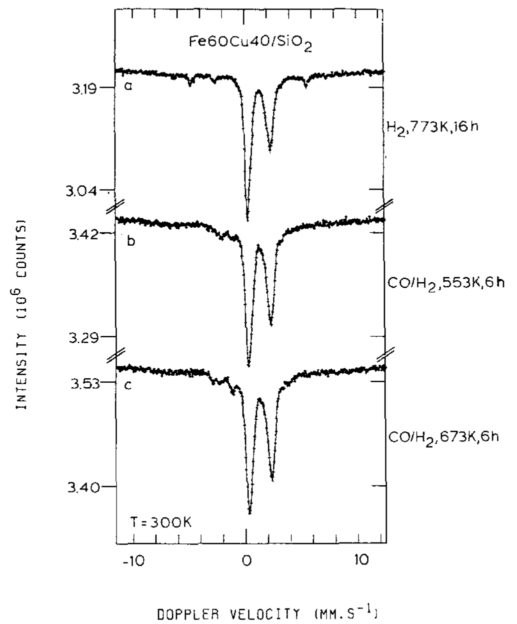

FIG. 4. Room temperature Mössbauer spectra of the Fe60Cu40 catalyst collected after the indicated treatments.

quenched from the above-mentioned reaction conditions are shown. The monometallic copper catalyst gives rise to a weak two-peak pattern (peak maxima at 875 and 1000 K). The carbided Fe–Cu (Fe80Cu20) and pure Fe catalysts give appreciably larger peaks. Electron micrographs of the bimetallic and pure iron catalysts taken prior to the TPH run show extensive filament growth, whereas no whiskers are observed with the pure copper catalyst. With the bimetallic catalysts the peak maxima shift to higher temperatures with increasing copper concentration. Furthermore, it appears that the peak area for Fe80Cu20 is greater than that of the monometallic iron catalyst. However, the peak area of Fe5Cu95 is appreciably smaller.

In Fig. 6 the amount of carbon (calculated from the peak area of the TPH profiles) per milligram catalyst is plotted as a function of the copper concentration. It can be seen that with increasing copper concentration the amount of deposited carbon drastically decreases. The lower carbon content of the pure Fe/SiO_2 catalyst compared to the iron-rich bimetallic catalysts arises from (i) the fact that the reduced iron particles are for the greater part encapsulated by the support (*21*) and (ii) from the lower degree of iron reduction (*17*).

The electron micrographs shown in Fig. 7 reveal the morphology of the whiskers grown in two bimetallic catalysts. In addition to thick filaments an appreciable amount of thin threads is also present (especially in the copper-rich catalyst). In some cases these whiskers appear to be clustered around the same metal particle. Bernardo *et al.* (*22*) have denoted this kind of filament "octopus" carbon and these thin filaments appear to be characteristic of the bimetallic catalysts. Although whisker growth does occur in the bimetallic catalyst, reactor plugging has not been observed with the copper-rich bimetallic catalysts. This indicates that the mechanical strength of such thin threads is considerably less than that of the thick filaments grown with monometallic iron particles (*6, 7*).

DISCUSSION

In the analysis of the activity and selectivity data of the bimetallic catalysts we will assume that the metal area per gram of

TABLE 1

Mössbauer Parameters Deduced from the Spectra in Fig. 4

Pretreatment	Iron species	IS[a] (mm/s)	QS (mm/s)	H_{eff} (kOe)	% area[b]
Fe60Cu40	Fe^{2+}	1.40	1.93		70
H_2, 16 h, 773 K	Fe^0	0.17			24
	Fe^0	0.31		318	5
Fe60Cu40	Fe^{2+}	1.34	1.85		74
CO/H_2, 6 h, 553 K	Fe^0	0.15			16
	ε'-$Fe_{2.2}C$	0.50		173	8
	θ-Fe_3C	0.45		212	2
Fe60Cu40	Fe^{2+}	1.34	1.90		77
CO/H_2, 6 h, 673 K	Fe^0	0.15			12
	ε'-$Fe_{2.2}C$	0.50		173	4
	θ-Fe_3C	0.45		212	7

[a] Isomer shift relative to sodium nitroprusside.

[b] Accuracy in relative area ±5%.

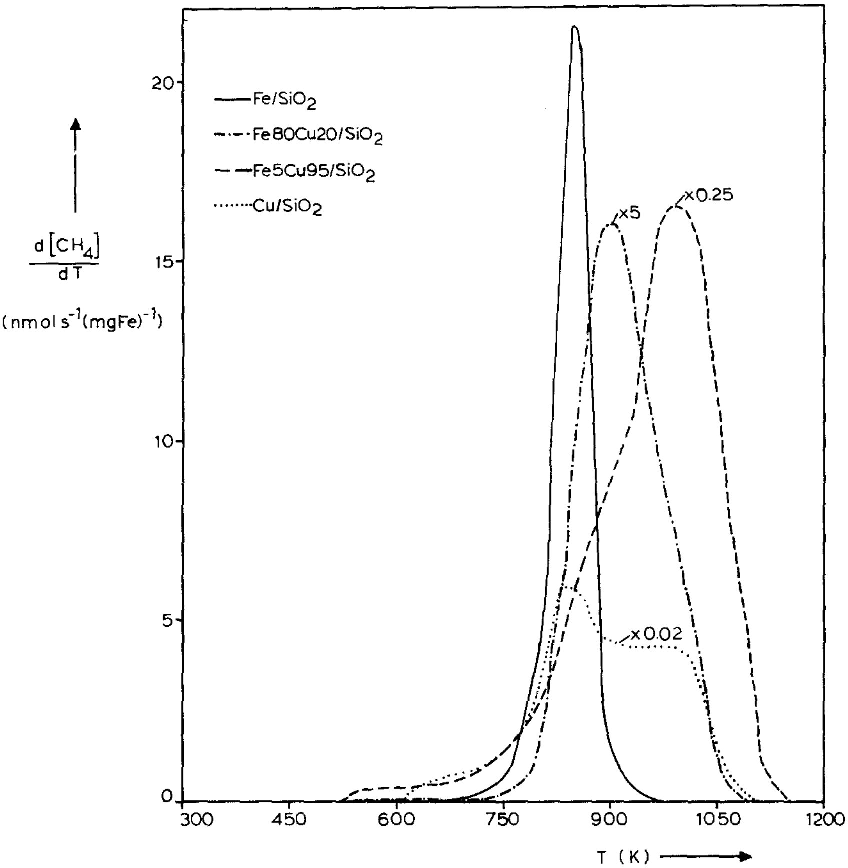

FIG. 5. TPH profiles of different catalysts carbided under identical conditions as described in the text. Multiplication with the indicated factors gives the measured profiles. With the pure copper catalyst the amount of deposited carbon is normalized on the amount of copper present.

metal is the same for all samples. This assumption is justified by transmission electron micrographs showing that in the reduced bimetallic catalysts the mean metal particle size is only slightly dependent on the overall composition (*17*).

The effect of copper on the hydrocarbon production rate can be appreciated from the results shown in Fig. 1. At low copper contents the activity of the bimetallic catalysts is markedly higher than that of the monometallic iron catalyst. Although the results show that with increasing copper content the activity decreases, it appears that the activity remains reasonably constant in the compositional range between 40 and 60 at.% copper. As is to be expected at high copper levels, the FT activity is virtually nil. In Part I (*17*) it was shown that the presence of copper markedly enhances the reducibility of the iron ions, thus explaining the higher hydrocarbon production rate of the iron-rich bimetallic catalysts compared to that of the monometallic catalysts. Mössbauer spectra of the reduced Fe–Cu catalysts showed that iron atoms are present as monometallic α-Fe particles and/or as small iron clusters in bimetallic Fe–Cu particles. On the basis of the Mössbauer spectra (Fig. 4) it appears that under the experimental conditions applied during the Fischer–Tropsch reaction both types of zero-valent iron atoms (partly) react to iron carbide. Apparently, under Fischer–

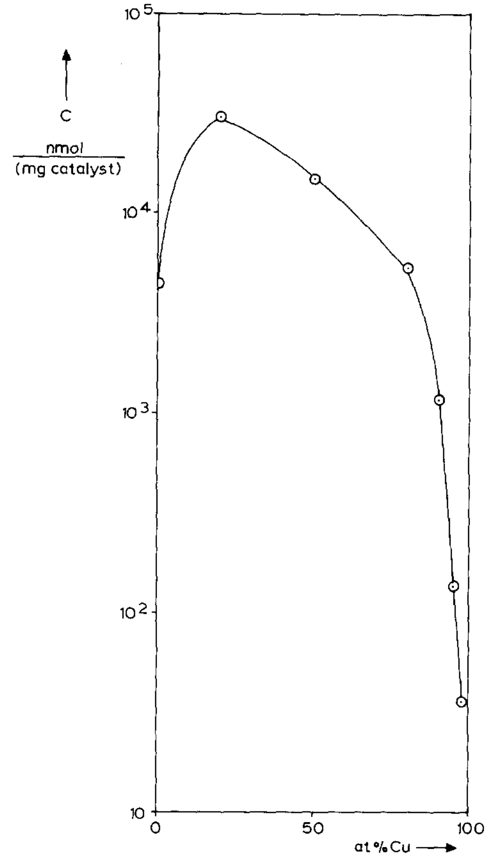

FIG. 6. The amount of deposited carbon as a function of the copper content.

Tropsch conditions copper does not prevent iron clusters present in a copper matrix to react to iron carbide. Previously, it was shown that carbon monoxide can induce at room temperature a significant iron enrichment in the surface of the bimetallic Fe–Cu particles (*17*). Therefore, it does not seem unreasonable to suggest that during the Fischer–Tropsch synthesis the iron–iron carbide concentration in the surface is appreciably higher than the iron–iron carbide bulk concentration of the bimetallic particle. In fact, it can be envisaged that the surfaces of the alloy particles consist of islets (or even a complete layer) of the active phase (iron–iron carbide). With increasing copper concentration the size of such islets will decrease, leading to a gradual decrease in activity. These features are schematically shown in Fig. 8. Accordingly, it can be explained that in the compositional range between 40 and 60 at.% copper the activity does not strongly depend on the overall composition.

The selectivity of the Fe60Cu40 catalyst for higher hydrocarbons is the same as that of the pure Fe catalyst. Fig. 3 shows that marked changes in the selectivity are only observed at higher copper concentrations, supporting the concept that at low copper contents the copper atoms are covered by iron–iron carbide islets. With increasing copper concentration both the CO_2 and CH_4 selectivities increase, whereas the selectivity for ethene markedly decreases. Copper is known to be a very effective catalyst for the water–gas shift reaction (*20, 23*) and as a result water produced in the FT reaction (proceeding on the iron–iron carbide islands) may react with carbon monoxide to carbon dioxide and hydrogen. The increase in the methane selectivity and the concomitant decrease in selectivity for the formation of olefins indicate that with increasing copper concentration hydrogenation reactions become more important. We have already reported (*17*) that at elevated temperatures copper becomes an active catalyst for hydrogen dissociation. Indeed, an increased supply of hydrogen atoms with increasing copper concentration can explain the observed selectivity changes. To summarize, the selectivity changes with iron–copper alloys at high copper levels are a result of an increasing contribution of two side reactions.

From Fig. 1 it appears that the rate of deactivation decreases with increasing copper concentration. Deactivation may result from an increasing amount of inactive carbon on the alloy surface. In general there will be a competition between hydrogenation and insertion of carbonaceous species, on the one hand, and a reaction between these species to inactive carbon, on the other hand. An enhanced hydrogenation

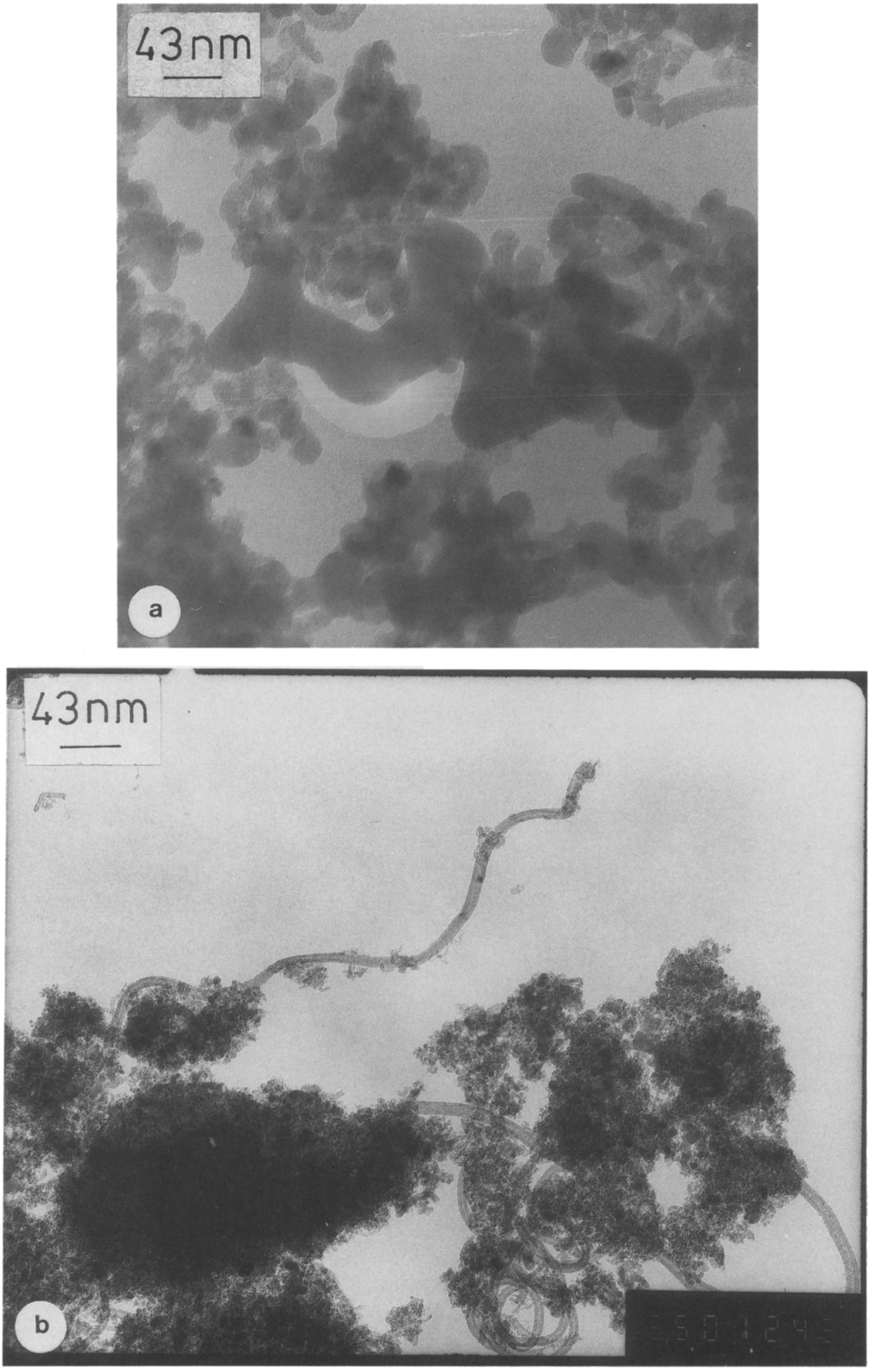

FIG. 7. Representative electron micrographs showing filamentous carbon in the carbided iron/copper catalysts: (a) Fe50Cu50, (b) Fe20Cu80.

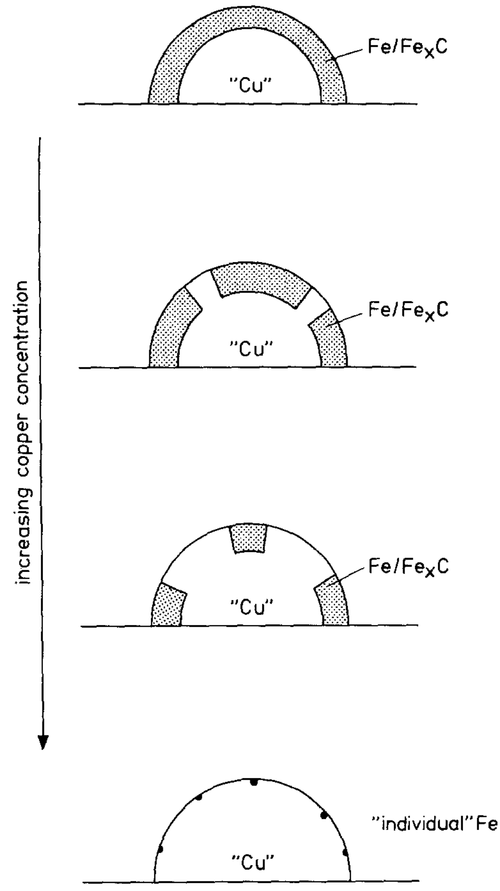

FIG. 8. Schematic representation of the bimetallic Fe–Cu particles under Fischer–Tropsch and carburization conditions.

function can also explain the decreasing rate of deactivation with increasing copper content.

The TPH experiments as well as the electron micrographs show that under the experimental conditions applied with the Fe–Cu catalysts filamentary carbon growth occurs. No whisker growth, however, is observed with the pure copper catalyst. This is to be anticipated from the mechanism accounting for the growth of such filaments (*6–8*). Briefly, it was shown that whisker growth occurs at the metal–support interface by a decomposing metastable metal carbide. As copper cannot react to carbide, filament growth is thus not expected with pure copper catalysts. On the other hand, filament growth with a pure iron catalyst is indeed observed. From Fig. 6 it appears that the amount of carbon in the carbided Fe–Cu alloys is even higher than in the monometallic iron catalyst (for reasons explained above).

Furthermore, the morphology of the fibers in the alloy samples has changed compared to the pure iron catalyst: the diameter of the whiskers has decreased and in some cases more whiskers are clustered around the same metal particle (octopus carbon). As has been discussed above, under Fischer–Tropsch conditions the surfaces of the bimetallic Fe–Cu particles probably consist of islets of the active iron phase (i.e., iron and iron carbide). The Mössbauer spectra show that with increasing severity of carbiding (i.e., a more elevated temperature) a greater amount of the iron clusters present in the copper matrix is transformed to iron carbide. The low solubility of iron carbide in copper (*24*) indicates that the interaction between iron carbide and copper is rather weak. Consequently, it can be envisaged that at the iron carbide–copper interface nucleation of filamentous carbon can occur. The dimensions of the iron–iron carbide islets dictate the diameter of the filaments, thus explaining the formation of extremely thin filaments. Furthermore, as more iron–iron carbide islands may be present on the alloy surface, more than one filament can grow on such a surface giving rise to the formation of "octopus" carbon. In addition, the mechanical strength of the filaments appears to decrease with decreasing thickness and as a result the structure of the catalyst does not deteriorate as a result of the growth of these thin filaments. At high copper contents the formation of whiskers is completely suppressed. It can be envisaged that with increasing copper content the iron atoms in the surface become more and more individualized and cannot be engaged to react to iron carbide. Thus, in order to suppress the growth of filamentous carbon the use of copper-rich bimetallic Fe–Cu catalysts seems to be advantageous.

CONCLUSIONS

(i) Iron–copper catalysts containing a small amount of copper exhibit a markedly higher activity in the Fischer–Tropsch reaction than monometallic iron catalysts. This is due to the fact that copper markedly enhances the reducibility of the iron ions and as a result a higher degree of iron reduction is obtained in the bimetallic catalysts. As is to be expected, however, with increasing copper content the activity decreases.

(ii) In a broad compositional range the selectivity is not affected by the presence of copper. At copper levels above 60 at.% the selectivity for carbon dioxide, methane, and paraffins (at the expense of olefins) increases. These results can be explained by assuming that with increasing copper content side reactions such as the water–gas shift reaction (producing carbon dioxide) and hydrogenation reactions (favouring production of methane and paraffins) become more important.

(iii) Under Fischer–Tropsch conditions not only the monometallic α-Fe particles but also the iron clusters present in the bimetallic Fe–Cu particles are (partly) converted to iron carbide, suggesting that both types of iron atoms are active in the Fischer–Tropsch reaction. It is argued that under Fischer–Tropsch conditions the surfaces of the bimetallic particles consist of iron–iron carbide islets, which explains why the effect of copper on selectivity becomes apparent at high copper levels only.

(iv) Growth of filamentary carbon proceeds not only on the monometallic iron particles but also on the iron–iron carbide islets present in the bimetallic particles, thus accounting for the formation of very thin whiskers and octopus carbon. At high copper contents whisker growth is suppressed.

ACKNOWLEDGMENTS

The authors are indebted to Dr. Ir. A. M. van der Kraan and Mr. E. Gerkema, Interfacultair Reactor Instituut, Delft University of Technology, for carrying out the Mössbauer experiments. The investigations were financially supported by the Netherlands Organization for the Advancement of Pure Research (SON/NWO).

REFERENCES

1. Anderson, R. B., *in* "Catalysis" (P. H. Emmett, Ed.), Vol. 4, p. 1. Reinhold, Baltimore (1956).
2. Dry, M. E., *in* "Catalysis, Science and Technology" (J. R. Anderson and M. Boudart, Eds.), Vol. 1, p. 159. Springer-Verlag, Berlin (1981).
3. Raupp, G. B., and Delgass, W. N., *J. Catal.* **58,** 361 (1979).
4. Amelse, J. A., Butt, J. B., and Schwartz, L. H., *J. Phys. Chem.* **82,** 558 (1978).
5. Niemantsverdriet, J. W., van der Kraan, A. M., van Dijk, W., and van der Baan, H. S., *J. Phys. Chem.* **84,** 3363 (1980).
6. de Bokx, P. K., Kock, A. J. H. M., Klop, W., Boellaard, E., and Geus, J. W., *J. Catal.* **96,** 454 (1985).
7. Kock, A. J. H. M., de Bokx, P.K., Boellaard, E., Klop, W., and Geus, J. W., *J. Catal.* **96,** 468 (1985).
8. Boellaard, E., Kock, A. J. H. M., de Bokx, P. K., and Geus, J. W., *J. Catal.* **96,** 481 (1985).
9. Ponec, V., *in* "Advances in Catalysis" (D. D. Eley, Herman Pines, and Paul B. Weisz, Eds.), Vol. 32, p. 149. Academic Press, New York, 1983.
10. Ponec, V., *Coal Sci.* **3,** 1 (1984).
11. Ponec, V., *Int. J. Quantum Chem.* **12**(2), 1 (1977).
12. van Barneveld, W. A. A., and Ponec, V., *J. Catal.* **89,** 542 (1984).
13. Shah, Y. T., and Perrotta, A. J., *Ind. Eng. Chem. Prod. Res. Dev.* **15,** 123 (1976).
14. Wachs, I. E., Dwyer, D. J., and Iglesia, E., *Appl. Catal.* **12,** 201 (1984).
15. US Patent 644,313 (1975).
16. Deutsches Patentschrift 923127 (1955); Deutsches Patentschrift 937706 (1956).
17. Wielers, A. F. H., Hop, C. E. C. A., van Beijnum, J., van der Kraan, A. M., and Geus, J. W., *J. Catal.* **121,** 364–374 (1990).
18. Smith, J. M., *in* "Chemical Engineering Kinetics," 3rd ed. McGraw–Hill, New York, 1981.
19. Kuijpers, E. G. M., Tjepkema, R. B., and Geus, J. W., *J. Mol. Catal.* **25,** 241 (1984).
20. Vannice, M. A., *in* "Catalysis, Science and Technology," (J. R. Anderson and M. Boudart, Eds.), Vol. 3, Chap. 3. Springer-Verlag, Berlin, 1982.
21. Wielers, A. F. H., Kock, A. J. H. M., Hop, C. E. C. A., Geus, J. W., and van der Kraan, A. M., *J. Catal.* **117,** 1 (1989).
22. Bernardo, C. A., Alstrup, I., and Rostrup-Nielsen, J. R., *J. Catal.* **96,** 517 (1985).
23. Kuijpers, E. G. M., Tjepkema, R. B., van der Wal, W. J. J., Mesters, C. M. A. M., Spronck, S. F. G. M., and Geus, J. W., *Appl. Catal.* **25,** 139 (1986).
24. Parameswaran, K., Metz, K., and Morris, A., *Metall. Trans. A.* **10A,** 1929 (1979).